Dipolar dephasing for structure determination in a paramagnetic environment

Article *in* Solid State Nuclear Magnetic Resonance · March 2021

DOI: 10.1016/j.ssnmr.2021.101728

Solid State Nuclear Magnetic Resonance 113 (2021) 101728

Contents lists available at ScienceDirect

Solid State Nuclear Magnetic Resonance

journal homepage: www.elsevier.com/locate/ssnmr

Dipolar dephasing for structure determination in a paramagnetic environment

Rubin Dasgupta, Karthick B.S.S. Gupta, Derek Elam [1], Marcellus Ubbink, Huub J.M. de Groot *

Leiden University, Leiden Institute of Chemistry, Gorlaeus Laboratories, Einsteinweg, 55 2333 CC, Leiden, the Netherlands

ARTICLE INFO

Keywords:
Cu(II)-(DL-Ala)$_2$.H$_2$O
REDOR
Shifted-REDOR
Paramagnetic solid-state NMR
Dipolar coupling

ABSTRACT

We demonstrate the efficacy of the REDOR-type sequences in determining dipolar coupling strength in a paramagnetic environment. Utilizing paramagnetic effects of enhanced relaxation rates and rapid electronic fluctuations in Cu(II)-(DL-Ala)$_2$.H$_2$O, the dipolar coupling for the methyl C–H that is 4.20 Å (methyl carbon) away from the Cu^{2+} ion, was estimated to be 8.8 ± 0.6 kHz. This coupling is scaled by a factor of ~0.3 in comparison to the rigid limit value of ~32 kHz, in line with partial averaging of the dipolar interaction by rotational motion of the methyl group. Limited variation in the scaling factor of the dipolar coupling strength at different temperatures is observed. The C–H internuclear distance derived from the size of the dipolar coupling is similar to that observed in the crystal structure. The errors in the dipolar coupling strength observed in the REDOR-type experiments are similar to those reported for diamagnetic systems. Increase in resolution due to the Fermi contact shifts, coupled with MAS frequencies of 30–35 kHz allowed to estimate the hyperfine coupling strengths for protons and carbons from the temperature dependence of the chemical shift and obtain a high resolution ^{1}H–^{1}H spin diffusion spectrum. This study shows the utility of REDOR-type sequences in obtaining reliable structural and dynamical information from a paramagnetic complex. We believe that this can help in studying the active site of paramagnetic metalloproteins at high resolution.

1. Introduction

Paramagnetic solid-state NMR has undergone a revolution in the past decade due to the development of high spinning frequency probes and tailored pulse sequences. Studying the ligands that directly coordinate the paramagnetic metal ions with NMR can provide insight into the structure and dynamics of the system [1–4]. Among the various interactions, dipolar interactions are attractive for characterizing fast cooperative dynamics that can be measured using rotational-echo, double resonance (REDOR) type solid state NMR experiments including shifted-REDOR for probing anisotropic motions [5–7].

In this study we show that rapid paramagnetic fluctuations favorably affect REDOR and shifted REDOR experiments therefore, those can be performed with high sensitivity and resolution. We find that internuclear dipolar couplings can be determined with high accuracy that is comparable to what has been achieved for diamagnetic systems. We have selected Cu(II)-(DL-Ala)$_2$.H$_2$O (Fig. 1) as a model system to test the utility of the REDOR type sequences and to probe the C–H dipolar coupling of the methyl group in the alanine ligand, which is directly coordinating the paramagnetic metal center [8–11]. Recently, well-resolved heteronuclear dipolar correlation spectroscopy was reported for Cu(II)-(DL-Ala)$_2$.H$_2$O [10,12–14]. The possibility to sustain internuclear dipolar transfer in the immediate vicinity of paramagnetic ions can be attributed to rapid paramagnetic fluctuations that average the anisotropic and traceless electron-nuclear dipolar interactions while leaving the isotropic contact shifts unaffected. Here, the *J*-coupling between the copper ions determines the fluctuation frequencies for averaging dipolar couplings, which are traceless without isotropic component and is intrinsic to a one-dimensional chain. This results in the motional narrowing from spin waves running along the chain [15]. This opens up a window of opportunity, since essential advantages of paramagnetism, such as rapid acquisition and increased spectral dispersion can be combined with the power of dipolar correlation spectroscopy for resolving static or dynamic structure quantitatively. To demonstrate this, we implement a REDOR method for Cu(II)-(DL-Ala)$_2$.H$_2$O by adapting the REDOR refocusing period to the fast rotation needed for signal detection in paramagnetic systems with their enhanced relaxation that limits the acquisition time. The Cu(II)-(DL-Ala)$_2$.H$_2$O form 1-dimensional chains in which the Cu^{2+}

* Corresponding author.
E-mail address: groot_h@lic.leidenuniv.nl (H.J.M. de Groot).
[1] Current address: BASF SE, RAA/OS-B7, Carl-Bosch-Strasse 38, 67056 Ludwigshafen am Rhein, Germany.

https://doi.org/10.1016/j.ssnmr.2021.101728
Received 24 January 2021; Received in revised form 26 February 2021; Accepted 26 February 2021
Available online 10 March 2021

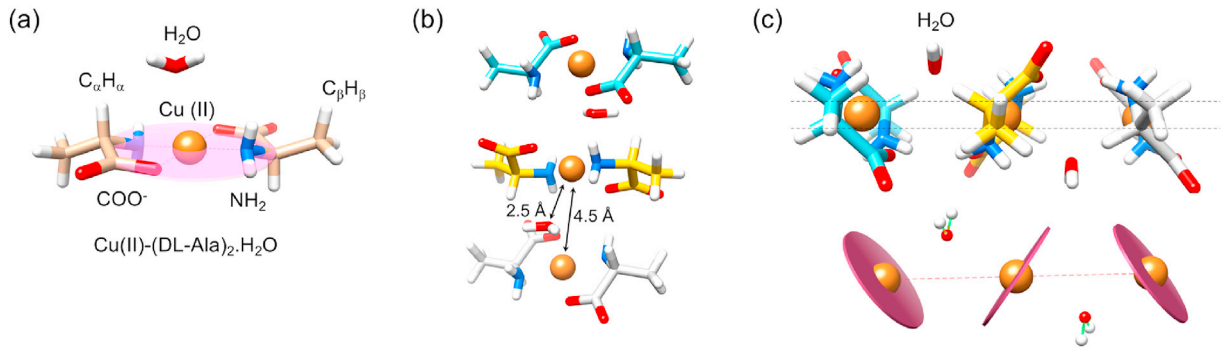

Fig. 1. Cu(II)-(DL-Ala)$_2$.H$_2$O crystal structure (cif:1153761) [8]. (a) Monomer depicting the plane of coordination and the respective proton and carbon orientations; (b) Trimeric representation of chain with distances between copper ions and between copper and oxygen of water; (c) Coordination plane of copper ions and position of water molecules.

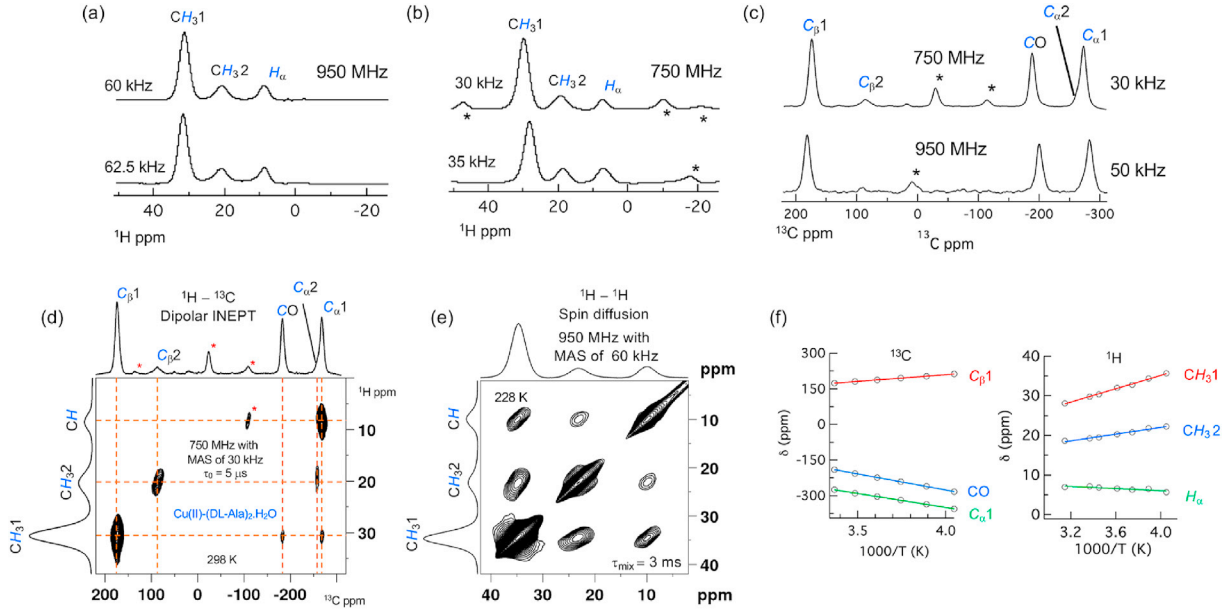

Fig. 2. (a) 1D ^{1}H rotor synchronized Hahn-echo spectra at MAS frequencies of 60 and 62.5 kHz in an external magnetic field of 22.31 T (950 MHz); (b) 1D ^{1}H rotor synchronized Hahn-echo spectra at MAS frequencies of 30 and 35 kHz in an external magnetic field of 17.6 T (750 MHz); (c) 1D^{13}C rotor synchronized Hahn-echo spectra at MAS frequencies of 30 and 50 kHz in an external magnetic field of 17.6 T and 22.31 T respectively; (d) The 2D ^{1}H–^{13}C dipolar-INEPT spectra at a MAS frequency of 30 kHz in an external magnetic field of 17.6 T with a transfer delay τ_0 of 5 μs at 298 K; (e) 2D ^{1}H–^{1}H spin diffusion at a MAS frequency of 60 kHz in an external magnetic field of 22.31 T with a mixing time τ_{mix} of 5 ms at 228 K; (f) Temperature dependence of the chemical shift for carbon and protons where C*H*$_3$1 and C$_\beta$ are in red, C*H*$_3$2 and carbonyl carbon CO are in blue and H$_\alpha$ and C$_\alpha$ are in green. Solid lines are the fit to equation (9). Spinning side bands in the panels showing spectra are marked with asterisks. The assignments in panel (a) to (e) of ^{1}H and ^{13}C responses are shown in italics and blue color.

ions are weakly coupled [11]. The antiferromagnetic coupling $2J = -2.21$ cm^{-1} translates into a characteristic frequency of ~70 GHz for the electronic spin fluctuations [11]. The properties of enhanced relaxation and rapid averaging of electron-nuclear dipolar interactions by paramagnetic fluctuations that are much faster than the frequency scale of the heteronuclear dipolar coupling of ~10 kHz or less, allow to perform heteronuclear dipolar recoupling experiments with fast MAS in a very short time, much shorter than for diamagnetic species. In addition, we show how ^{1}H–^{1}H spin diffusion spectra and the temperature dependence of proton and carbon shifts from 1D Hahn-echo experiments can help to collect structural information from paramagnetic systems with ultra-fast MAS.

2. Experimental procedures

2.1. Sample preparation and solid-state NMR experiments

Cu(II)-(DL-Ala)$_2$.H$_2$O complex was synthesized as reported earlier [10]. All chemicals including the uniformly labelled ^{13}C-DL-alanine were obtained from Sigma Aldrich (USA).

Solid-state NMR experiments were performed with AV-I (17.6 T) 750 MHz and AV-HDIII (22.31 T) 950 MHz spectrometers equipped with a 2.5 mm and 1.3 mm MAS probe, respectively, at spinning frequencies ranging from 30 to 62.5 kHz 1D proton and carbon spectra were recorded with a rotor synchronized Hahn-echo sequence (Fig. S4a). The high-power $\pi/2$ pulses were 2 μs and 2.5 μs for ^{1}H and ^{13}C, respectively. A dead time of 4.5 μs was subtracted from the refocusing period in the Hahn-echo pulse sequence. A comparison of spectra obtained with single 90° pulse (Fig. S1) with rotor synchronized Hahn-echo spectra (Fig. 2) confirms that there is little phase distortion in echo spectra obtained with a large spectral window (SW) [4]. The advantage of using rotor-synchronized Hahn-echo over single 90° pulse is elimination of probe artifacts as observed from Fig. S1a and Fig. 2a. This prompted us to use rotor-synchronized Hahn-echo pulse sequence to obtain 1D spectra for both carbon and proton for further study.

The 1D and 2D dipolar-INEPT sequence was adopted from

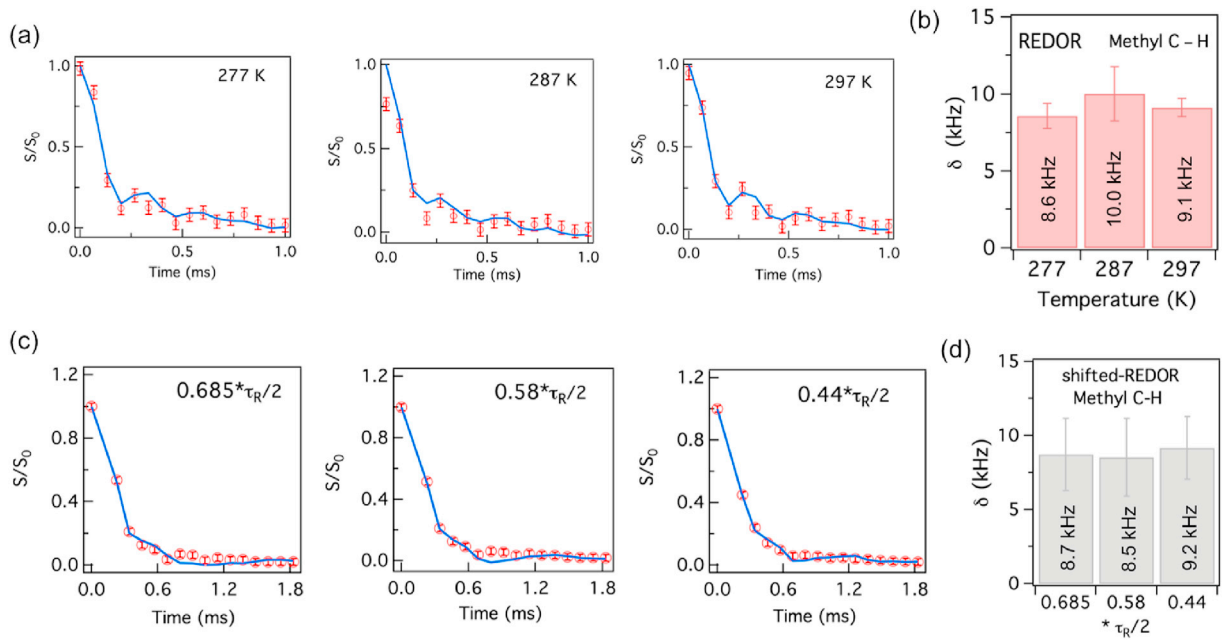

Fig. 3. (a) REDOR curve for methyl C–H ($C_\beta 1$ and $CH_3 1$) in Cu(II)-(DL-Ala)$_2$.H$_2$O at 277 K, 287 K and 297 K, the solid lines represent the fit; (b) The dipolar coupling strength estimated from fitting the REDOR curve for the methyl C–H ($C_\beta 1$ and $CH_3 1$); (c) Shifted-REDOR curves at a MAS frequency of 30 kHz with different shift of the π pulse from ideal $\tau_R/2$ (16.67 μs). The solid blue lines are fit with asymmetric parameter η value of 0.1; (d) Dipolar coupling strength estimated from the shifted-REDOR curve fit of methyl C–H ($C_\beta 1$ and $CH_3 1$).

Wickramasinghe et al. (2006) with a $\pi/2$ pulse length similar to the rotor synchronized Hahn-echo experiment [13]. Temperature dependent experiments were performed at temperatures between 247 K and 318 K. For the 2D ^{1}H–^{1}H spin diffusion (Fig. S4b) experiment the mixing time was varied from 1 ms to 5 ms with a total acquisition time of 530 μs and a delay of 30 ms between scans. 200 slices of data were acquired in the t1 dimension in a total experiment time of <5 min. REDOR and shifted-REDOR data were collected by direct excitation of ^{13}C (Figs. S4c and S4d) [5,6,16–18]. The $\pi/2$ pulse lengths were 2 μs and 2.2 μs for ^{1}H and ^{13}C respectively. Temperature calibration was done using samarium tin oxide and lead nitrate [19–21]. Data analysis was performed with TOPSPIN 4.0.5 (Bruker) and Igor pro 6.37.

2.2. REDOR and shifted-REDOR data analysis

The REDOR and shifted-REDOR curves were fitted with SIMPSON 4.2.1 [22,23]. The geometry of Cu(II)-(DL-Ala)$_2$.H$_2$O was adopted from Calvo et al. (1991) and Zhang et al. (2005) to generate the spin system parameters, dipolar coupling and Euler angles using SIMMOL-VMD [8, 24–26]. The signal from the methyl C–H was used as a reporter to determine the dipolar coupling strength due to its intrinsic isotropic motion and high S/N ratio (Fig. 2a and b). The fitting algorithm as implemented in SIMPSON package was used to estimate the dipolar coupling [22–24].

The rigid limit dipolar coupling strength of the methyl C–H is ~32.1 kHz which corresponds to an internuclear distance of 0.98 Å [26]. It is known that methyl rotation partially averages the dipolar coupling between the C–H bond of the methyl group and therefore the rigid limit dipolar coupling is scaled according to [27,28].

$$D_{avg} = S^{*}D, \tag{1}$$

with D the dipolar coupling strength in the rigid limit. The scaling factor is

$$S = \left(3\cos^2\theta - 1\right)/2, \tag{2}$$

where θ is the angle between the methyl C–H and the rotational axis, which in this case is the bond between $C_\alpha - C_\beta$. For a tetrahedral geometry of the methyl group $\theta = 109.5°$. This gives a theoretical scaling factor of $S = 0.333$ (Fig. S5) and $D_{avg} = 10.69$ kHz for the C–H bond in Cu(II)-(DL-Ala)$_2$.H$_2$O in the rotating methyl group. For the analysis of the data, the scaled $D_{avg} = 10.69$ kHz was changed to fit the experimental data. The average dipolar coupling strength was optimized to fit the REDOR curve using the fitting algorithm of SIMPSON. The homonuclear dipolar coupling between the three protons of the methyl group was also scaled by the theoretical value of 0.333 to give a $D_{avg} = 9.76$ kHz [26]. The codes for fitting and to obtain the spin-system can be downloaded from zenodo.org (https://doi.org/10.5281/zenodo.4599603).

2.3. Theory of temperature dependence of Fermi contact shifted resonances

The chemical shift of the paramagnetic system is temperature dependent and the observed chemical shift is given by [29].

$$\delta_{obs} = \delta_{dia} + \delta_{FCS} + \delta_{PCS}, \tag{3}$$

where δ_{dia} is the diamagnetic chemical shift and δ_{FCS}, δ_{PCS} are the contributions from the Fermi contact shift (FCS) and pseudo-contact shift (PCS) respectively [29,30]. For the nuclei of coordinating ligands FCS ≫ PCS and eq. (1) can be written as

$$\delta_{obs} \approx \delta_{dia} + \delta_{FCS} \tag{4}$$

The contribution from the FCS is given by [30].

$$\delta_{FCS} = \frac{AS_z}{\hbar\gamma_I B_0}, \tag{5}$$

with $A = \frac{2}{3}\hbar\gamma_I\mu_B g_e\mu_0\rho$, the isotropic hyperfine coupling that is proportional to the spin density ρ on a nucleus. The S_z is the expectation value of the z magnetization, $\hbar$ is the reduced Planck constant, γ_I is the gyromagnetic ratio of the nucleus in question, and B_0 is the external magnetic field.

Since the S_z is related to the magnetic susceptibility according to [30, 31].

$$S_z = \frac{B_0 \chi}{\mu_B g_e \mu_0}, \tag{6}$$

where μ_B is the Bohr magneton, $g_e \approx 2.003$ is the free electron g-value, and μ_0 is the permeability of the vacuum, the FCS can also be expressed in terms of the magnetic susceptibility χ by

$$\delta_{FCS} = \frac{A\chi}{\hbar \gamma_I \mu_B g_e \mu_0}. \tag{7}$$

The system is a linear chain in the high temperature limit, since $2J = -2.2\ cm^{-1}$, which translates into ~ 3 K. Therefore, we are in the high temperature limit, $|2J| \ll T$, and the experiments for Cu(II)-(DL-Ala)$_2$.H$_2$O were performed at this limit. The magnetic susceptibility is then given by [32].

$$\chi = \frac{S(S+1)\mu_B^2 g_e^2 \mu_0}{3k_B T}, \tag{8}$$

where $S = 1/2$ is the spin of the Cu(II) ion, k_B is the Boltzmann constant and T is the temperature in Kelvin.

Substituting eq. (8) in eq. (7), eq. (4) can be written as

$$\delta_{obs} \approx \delta_{dia} + A\frac{S(S+1)\mu_B g_e}{3\hbar \gamma_I k_B T} \tag{9}$$

for the temperature dependent chemical shift, which was used to determine hyperfine coupling constant by fitting to the data in Fig. 3.

3. Results and discussion

3.1. NMR characterization of Cu(II)-(DL-Ala)$_2$.H$_2$O

There are several advantages when working with Cu(II) paramagnetic systems. Since Cu(II) has small susceptibility the Fermi-contact interaction is stronger than the paramagnetic relaxation enhancement (PRE) [29]. This results in a better resolution because of the increase in the spectral dispersion without adversely affecting the linewidth. Additionally, reduction of experimental time due to fast longitudinal relaxation compared to diamagnetic systems can be achieved. In contrast, with other metal ions such as Tb(III) the susceptibility anisotropy is large and may lead to resonances broadened beyond detection due to increase in PRE-effects [29]. Fig. 2 shows the 1D spectra of ^{1}H and ^{13}C at different spinning frequencies and magnetic fields. The resolution is enhanced by the paramagnetic shifts at very fast MAS (>20 kHz) [12–14,33–35].

The 1D ^{1}H rotor-synchronized Hahn-echo spectra (Fig. 2a and b) show three prominent resonances attributed to CH_α at 8 ppm and C$H_3$1 at 32 ppm and C$H_3$2 at 21 ppm. We observed that the intensity of C$H_3$1 is 4 times that of H_α and C$H_3$2, while H$_\alpha$ and C$H_3$2 show similar intensities. The carbon spectrum shows three prominent resonances for C_α1 at −280 ppm, CO at −200 ppm and C_β1 at 180 ppm and two minor resonances for C_α2 at −258 ppm and C_β2 at 88 ppm (Fig. 2c and d and Table S1) [10,13,35]. The two components were attributed to two orientations of the methyl group as a consequence of crystal packing, where the major component (C$H_3$1/C_β1) is closer to the copper ion, while the minor component (C$H_3$2/C_β2) is more distant [8,36]. The ^{1}H signals from the NH$_2$ group (data not shown) were reported to be at −132.7 and −159.5 ppm [10]. The ^{1}H from the water molecule are generally broadened beyond detection due to fast exchange dynamics [10,35]. The methyl group of the major component was reported to be undergoing fast rotation which results in a single resonance for the three methyl protons (Fig. 2a and b) [10].

A dipolar-INEPT experiment was performed to check the quality of the sample and the efficiency of polarization transfer via dipolar interactions, which was previously shown to be superior to cross polarization based transfer for paramagnetic systems [13,37]. The spectrum is similar to the one reported earlier (Fig. 2d), albeit with better resolution and S/N, allowing to identify the splitting of the methyl group response that arises due to crystal packing effects [8,13,36].

Table 1
Dipolar coupling strength between C–H (C_β1 and C$H_3$1) at different temperatures using REDOR with a MAS frequency of 30 kHz.

Temp (K)	δ kHz	Scaling factor	Methyl C–H (C_β1 and C$H_3$1) distance (Å)
277	8.6 ± 0.8	0.29 ± 0.03	1.1 ± 0.1
287	10.0 ± 1.7	0.34 ± 0.06	1.0 ± 0.2
297	9.1 ± 0.6	0.32 ± 0.02	1.0 ± 0.1

The 2D ^{1}H–^{1}H spin diffusion spectra acquired at 22.31 T with a MAS frequency of 60 kHz (Figs. 2e and S3), show that a high resolution homonuclear 2D spectrum can be obtained under paramagnetic conditions with modification of the pulse sequence to consider the paramagnetic effects of increased relaxation and rapid fluctuations. Similar observations were reported for copper cyclam complexes [37].

The temperature dependence of the chemical shift shows strong Curie behavior for CO, C_α1, C_β1, C$H_3$1 and C$H_3$2 while weak anti-Curie behavior is observed for H$_\alpha$ (Fig. 2f and Fig. S2a). The hyperfine coupling strengths are summarized in Table S2, obtained after fitting the data with equation (9) (Fig. 2f) [38]. It is interesting to observe that, although the H$_\alpha$ is close to the copper, the hyperfine coupling constant and hence the spin density on it is less than for H$_\beta$. This was also observed in DFT calculations for Cu(II)-(DL-Ala)$_2$.H$_2$O showing very little electron density localized on the H$_\alpha$ atom [26,38]. The sign of the hyperfine coupling strength provides the spin polarization of the electron on the nucleus with respect to the external magnetic field. It was observed to be parallel for C_β1, C$H_3$1 and C$H_3$2 and anti-parallel for C_α1, CO and H$_\alpha$ (Table S2 and Fig. 2f). These observations are in line with the calculations performed on copper alanine complexes and previously reported data (Table S3) [38]. The estimated δ_{dia} from the fit of the temperature dependencies of the chemical shift (Fig. 2f) is summarized in Table S2. They differ from the expected diamagnetic chemical shift of DL-alanine (Table S4). This difference can be attributed to the differences in crystal packing of Cu(II)-(DL-Ala)$_2$.H$_2$O and DL-alanine (Fig. S6). The NMR chemical shift tensor for small molecules in solid state NMR differs significantly between different crystal forms due to changes in hydrogen bonding, stacking, ring current, C–H···π interactions etc. [39] DFT calculations of different crystal forms of purine derivatives show that the change in the diamagnetic chemical shift can be as high as 6.5 ppm, 20 ppm and 55 ppm for proton, carbon and nitrogen respectively [39].

The full width at half of the maximum (FWHM) of the resonances decreases with increasing temperature (Figs. S2b and S2c). Most likely, an increase in the electronic relaxation rate with temperature reduces the paramagnetic relaxation enhancement.

3.2. Dipolar coupling strength estimation

Dipolar coupling measurements can provide insight into the dynamics of the molecule [5,40]. Here, we have employed REDOR (Fig. S4c) and shifted-REDOR (Fig. S4d) to measure the dipolar coupling between ^{1}H and ^{13}C of the methyl group in Cu(II)-(DL-Ala)$_2$.H$_2$O [5,6]. The choice of these pulse sequences was based on their robustness for amplitude mis-setting, inhomogeneities in the radiofrequency field, carrier offset and CSA [5]. The methyl group was used as a probe because of the presence of intrinsic methyl rotation that partially averages the dipolar coupling and its higher S/N ratio compared to that of other protons (Fig. 2a and b).

Fig. 3a shows the ^{1}H–^{13}C REDOR curves of the C–H in C$H_3$1 group at 277 K, 287 K and 297 K obtained at a MAS frequency of 30 kHz. The dipolar coupling strengths estimated after the fitting are 8.6 kHz, 10.0 kHz and 9.2 kHz respectively (Table 1 and Fig. 3b). These values correspond with a scaling factor of ~0.3 (Table 1) relative to the rigid limit value of ~32 kHz, consistent with previously reported data for alanine in the diamagnetic crystalline state and similar to the theoretical scaling factor of 0.333 [27]. The accuracy of the paramagnetic measurement is

Table 2
Dipolar coupling strength of methyl C–H ($C_\beta 1$ and $CH_3 1$) using shifted-REDOR and at different fraction of $\tau_R/2$ by which the π pulse is shifted at MAS frequency of 35 kHz.

Fraction of $\tau_R/2$ shift	δ kHz	Scaling factor	Methyl C–H ($C_\beta 1$ and $CH_3 1$) distance (Å)
0.685	8.7 ± 2.4	0.30 ± 0.08	1.0 ± 0.3
0.580	8.5 ± 2.6	0.29 ± 0.09	1.1 ± 0.3
0.440	9.2 ± 2.1	0.32 ± 0.07	1.0 ± 0.2

similar to that reported for the diamagnetic systems [5,6].

The corresponding internuclear ^1H–^{13}C ($C_\beta 1$ and $CH_3 1$) distances derived after dividing the dipolar coupling strength with the scaling factor is ~1.0 Å (Table 1) which is very similar to the crystal structure (1.0 Å) [8,26]. This demonstrates the efficacy of the REDOR sequence in obtaining reliable distance information in a paramagnetic system. It is noteworthy that although the paramagnetic shift is temperature dependent the dipolar coupling strength is preserved. This property can be explored to characterize the dipolar coupling strength between the nuclei in the vicinity of the metal at the active site of the paramagnetic metalloproteins and consequently get insight into the dynamics.

It was recently reported that using a variant of REDOR where the π pulses are shifted from its original position, known as shifted-REDOR (Fig. S4d), is able to identify anisotropic motions present in the protein via the asymmetry parameter η [5,6]. We investigated the dephasing behavior in the presence of the paramagnetic metal center at a spinning frequency of 30 kHz and at 297 K with the π pulse shift (τ_S) of 0.685 or 0.58 or 0.44 times $\tau_R/2$ (Fig. 3c). The dipolar coupling strength between the methyl C–H nuclei does not change with varying τ_s and it matches with the values obtained from REDOR (Tables 1 and 2). The derived internuclear distance is ~1.0 Å (Table 2), consistent with the crystal structure and similar to REDOR. Hence, shifted-REDOR appears also robust and reliable for obtaining structural information. The asymmetry parameter η of 0.1 gave the best fit, which is in line with the lack of anisotropic motion in the methyl group rotation. While there was no anomaly in the implementation of shifted-REDOR for Cu(II)-(DL-Ala)$_2$.H_2O, in shifted-REDOR (Fig. 3c), the oscillatory behavior observed in the REDOR (Fig. 3a) is diminished which can be due to the presence of additional protons (NH_2 and Hα). This is consistent with the observations of Schanda et al. (2011), who showed that the presence of additional protons near the observed nuclei reduces the oscillatory nature of the shifted-REDOR for ubiquitin crystals [5,6].

In summary, both REDOR and shifted-REDOR sequences provide reliable estimates of the dipolar coupling strength and consequently information about the structure and methyl rotation.

4. Conclusions

This study shows that high resolution ^1H based solid-state NMR spectra can be obtained for a paramagnetic system at fast MAS (>25 kHz). Using the high sensitivity of ^1H and the high resolution due to the paramagnetic nature of Cu(II), a temperature dependence study of the model compound Cu(II)-(DL-Ala)$_2$.H_2O could be performed that shows that the shift correlates with the spin delocalization over the ligands. The fast MAS has enabled the implementation of ^1H–^1H homonuclear spin diffusion, REDOR and shifted-REDOR pulse sequences. Our benchmark is the existing crystal structure. The error in the measured values were similar to that observed for diamagnetic systems and are largely systematic errors from e.g. thermal motions that effectively reduce the dipolar coupling from its rigid limit value. We present a technical step forward by showing that both REDOR and shifted-REDOR are quantitatively reliable in determining the dipolar coupling strength and internuclear distances near the paramagnetic metal center, which paves the way for future application in metalloproteins to probe fast dynamics. In addition, the results contribute to the converging and convincing evidence that paramagnetic solid-state NMR is increasingly accessible and can be interpreted in the same way as the NMR spectra of diamagnetic solids.

Declaration of competing interest

The authors declare that asethey have no known competing financial interests or personal relationships that could have appeared to influence the work reported in this paper.

Acknowledgment

This project was funded by Netherlands' Magnetic Resonance Research School (NWO-BOO 022.005.029). The use of ultrahigh-field nuclear magnetic resonance facility at Utrecht University was sponsored by uNMR-NL, the NWO-funded, national roadmap for the large-scale NMR facility in the Netherlands (grant number: 184-032-207). Prof. Thomas Vosegaard is gratefully acknowledged for discussions on the SIMPSON fitting procedure.

Appendix A. Supplementary data

Supplementary data to this article can be found online at https://doi.org/10.1016/j.ssnmr.2021.101728.

References

[1] G. Pintacuda, N. Giraud, R. Pierattelli, A. Böckmann, I. Bertini, L. Emsley, Solid-state NMR spectroscopy of a paramagnetic protein: assignment and study of human dimeric oxidized CuII–ZnII superoxide dismutase (SOD), Angew. Chem. Int. Ed. 46 (2007) 1079–1082, https://doi.org/10.1002/anie.200603093.
[2] I. Bertini, L. Emsley, M. Lelli, C. Luchinat, J. Mao, G. Pintacuda, Ultrafast MAS solid-state NMR permits extensive 13C and 1H detection in paramagnetic metalloproteins, J. Am. Chem. Soc. 132 (2010) 5558–5559, https://doi.org/10.1021/ja100398q.
[3] Gwendal Kervern, Guido Pintacuda, Yong Zhang, Eric Oldfield, Charbel Roukoss, Emile Kuntz, Eberhardt Herdtweck, Jean-Marie Basset, Sylvian Cadars, Anne Lesage, Christophe Copéret, Lyndon Emsley, Solid-State NMR of a Paramagnetic DIAD-FeII Catalyst: Sensitivity, Resolution Enhancement, and Structure-Based Assignments, 2006, https://doi.org/10.1021/ja063510n.
[4] A.J. Pell, G. Pintacuda, Broadband solid-state MAS NMR of paramagnetic systems, Prog. Nucl. Magn. Reson. Spectrosc. 84–85 (2015) 33–72, https://doi.org/10.1016/j.pnmrs.2014.12.002.
[5] P. Schanda, B.H. Meier, M. Ernst, Accurate measurement of one-bond H–X heteronuclear dipolar couplings in MAS solid-state NMR, J. Magn. Reson. 210 (2011) 246–259, https://doi.org/10.1016/j.jmr.2011.03.015.
[6] P. Schanda, M. Huber, J. Boisbouvier, B.H. Meier, M. Ernst, Solid-state NMR measurements of asymmetric dipolar couplings provide insight into protein side-chain motion, Angew. Chem. Int. Ed. 50 (2011) 11005–11009, https://doi.org/10.1002/anie.201103944.
[7] M.G. Jain, K.R. Mote, J. Hellwagner, G. Rajalakshmi, M. Ernst, P.K. Madhu, V. Agarwal, Measuring strong one-bond dipolar couplings using REDOR in magic-angle spinning solid-state NMR, J. Chem. Phys. 150 (2019), 134201, https://doi.org/10.1063/1.5088100.
[8] R. Calvo, P.R. Levstein, E.E. Castellano, S.M. Fabiane, O.E. Piro, S.B. Oseroff, Crystal structure and magnetic interactions in bis (D, L-alaninato) copper (II) hydrate, Inorg. Chem. 30 (1991) 216–220.
[9] A. Mirceva, J.O. Thomas, T. Gustafsson, Structure of trans-bis(dl-α-alaninato) copper(II) monohydrate, Acta Crystallogr. C 45 (1989) 1141–1144, https://doi.org/10.1107/S0108270189000788.
[10] K. Liu, D. Ryan, K. Nakanishi, A. McDermott, Solid state NMR studies of paramagnetic coordination complexes: a comparison of protons and deuterons in detection and decoupling, J. Am. Chem. Soc. 117 (1995) 6897–6906, https://doi.org/10.1021/ja00131a011.
[11] R. Calvo, R.P. Sartoris, H.L. Calvo, E.F. Chagas, R.E. Rapp, Antiferromagnetic spin chain behavior and a transition to 3D magnetic order in Cu(D,L-alanine)2: roles of H-bonds, Solid State Sci. 55 (2016) 144–151, https://doi.org/10.1016/j.solidstatesciences.2016.03.005.
[12] Y. Ishii, N.P. Wickramasinghe, S. Chimon, A new approach in 1D and 2D 13C high-resolution solid-state NMR spectroscopy of paramagnetic organometallic complexes by very fast magic-angle spinning, J. Am. Chem. Soc. 125 (2003) 3438–3439, https://doi.org/10.1021/ja0291742.
[13] N.P. Wickramasinghe, Y. Ishii, Sensitivity enhancement, assignment, and distance measurement in 13C solid-state NMR spectroscopy for paramagnetic systems under

fast magic angle spinning, J. Magn. Reson. 181 (2006) 233–243, https://doi.org/10.1016/j.jmr.2006.05.008.
[14] Y. Ishii, N.P. Wickramasinghe, 1H and 13C high-resolution solid-state NMR of paramagnetic compounds under very fast magic angle spinning, in: Mod. Magn. Reson., Springer, Dordrecht, 2008, pp. 467–474, https://doi.org/10.1007/1-4020-3910-7_59.
[15] A.C. Kolbert, R. Verel, H.D. Groot, M. Almeida, Determination of the spin density distribution in the organic conductor DMTM(TCNQ)2 with 13C magic angle spinning NMR, Mol. Phys. 91 (1997) 725–730, https://doi.org/10.1080/002689797171210.
[16] C.P. Jaroniec, B.A. Tounge, C.M. Rienstra, J. Herzfeld, R.G. Griffin, Recoupling of heteronuclear dipolar interactions with rotational-echo double-resonance at high magic-angle spinning frequencies, J. Magn. Reson. 146 (2000) 132–139, https://doi.org/10.1006/jmre.2000.2128.
[17] J. Schaefer, "Development of REDOR rotational-echo double-resonance NMR" by terry gullion and jacob schaefer, J. Magn. Reson. 81 (1989) 196–200, https://doi.org/10.1016/j.jmr.2011.08.012.
[18] R. Gertman, I. Ben Shir, S. Kababya, A. Schmidt, In situ observation of the internal structure and composition of biomineralized emiliania huxleyi calcite by solid-state NMR spectroscopy, J. Am. Chem. Soc. 130 (2008) 13425–13432, https://doi.org/10.1021/ja803985d.
[19] A.E. Aliev, K.D.M. Harris, Simple technique for temperature calibration of a MAS probe for solid-state NMR spectroscopy, Magn. Reson. Chem. 32 (1994) 366–369, https://doi.org/10.1002/mrc.1260320611.
[20] X. Guan, R.E. Stark, A general protocol for temperature calibration of MAS NMR probes at arbitrary spinning speeds, Solid State Nucl. Magn. Reson. 38 (2010) 74–76, https://doi.org/10.1016/j.ssnmr.2010.10.001.
[21] B. Langer, I. Schnell, H.W. Spiess, A.-R. Grimmer, Temperature calibration under ultrafast MAS conditions, J. Magn. Reson. 138 (1999) 182–186, https://doi.org/10.1006/jmre.1999.1717.
[22] M. Bak, J.T. Rasmussen, N.C. Nielsen, SIMPSON: a general simulation program for solid-state NMR spectroscopy, J. Magn. Reson. 147 (2000) 296–330, https://doi.org/10.1006/jmre.2000.2179.
[23] Z. Tošner, R. Andersen, B. Stevensson, M. Edén, N.Chr Nielsen, T. Vosegaard, Computer-intensive simulation of solid-state NMR experiments using SIMPSON, J. Magn. Reson. 246 (2014) 79–93, https://doi.org/10.1016/j.jmr.2014.07.002.
[24] T. Vosegaard, A. Malmendal, N.C. Nielsen, The flexibility of SIMPSON and SIMMOL for numerical simulations in solid-and liquid-state NMR spectroscopy, Monatshefte Für Chem. Chem. Mon. 133 (2002) 1555–1574, https://doi.org/10.1007/s00706-002-0519-2.
[25] M. Bak, R. Schultz, T. Vosegaard, N. Chr, Nielsen, specification and visualization of anisotropic interaction tensors in polypeptides and numerical simulations in biological solid-state NMR, J. Magn. Reson. 154 (2002) 28–45, https://doi.org/10.1006/jmre.2001.2454.
[26] Y. Zhang, H. Sun, E. Oldfield, Solid-state NMR Fermi contact and dipolar shifts in organometallic complexes and metalloporphyrins, J. Am. Chem. Soc. 127 (2005) 3652–3653, https://doi.org/10.1021/ja043461j.
[27] C.H. Wu, B.B. Das, S.J. Opella, 1H–13C hetero-nuclear dipole–dipole couplings of methyl groups in stationary and magic angle spinning solid-state NMR experiments of peptides and proteins, J. Magn. Reson. 202 (2010) 127–134, https://doi.org/10.1016/j.jmr.2009.10.007.
[28] S. Asami, B. Reif, Accessing methyl groups in proteins via 1 H-detected MAS solid-state NMR spectroscopy employing random protonation, Sci. Rep. 9 (2019) 1–13, https://doi.org/10.1038/s41598-019-52383-3.
[29] I. Bertini, C. Luchinat, G. Parigi, E. Ravera, NMR of Paramagnetic Molecules: Applications to Metallobiomolecules and Models, second ed., Elsevier, Amsterdam, 2017.
[30] I. Bertini, C. Luchinat, G. Parigi, Magnetic susceptibility in paramagnetic NMR, Prog. Nucl. Magn. Reson. Spectrosc. 40 (2002) 249–273.
[31] G.N. La Mar, G.R. Eaton, R.H. Holm, F.Ann Walker, Proton magnetic resonance investigation of antiferromagnetic oxo-bridged ferric dimers and related high-spin monomeric ferric complexes, J. Am. Chem. Soc. 95 (1973) 63–75, https://doi.org/10.1021/ja00782a012.
[32] E. Sinn, Magnetic exchange in polynuclear metal complexes, Coord. Chem. Rev. 5 (1970) 313–347, https://doi.org/10.1016/S0010-8545(00)80132-0.
[33] N.P. Wickramasinghe, M.A. Shaibat, C.R. Jones, L.B. Casabianca, A.C. de Dios, J.S. Harwood, Y. Ishii, Progress in C13 and H1 solid-state nuclear magnetic resonance for paramagnetic systems under very fast magic angle spinning, J. Chem. Phys. 128 (2008), 52210, https://doi.org/10.1063/1.2833574.
[34] N.P. Wickramasinghe, M. Shaibat, Y. Ishii, Enhanced sensitivity and resolution in 1H solid-state NMR spectroscopy of paramagnetic complexes under very fast magic angle spinning, J. Am. Chem. Soc. 127 (2005) 5796–5797, https://doi.org/10.1021/ja042188i.
[35] M.J. Willans, D.N. Sears, R.E. Wasylishen, The effectiveness of 1H decoupling in the 13C MAS NMR of paramagnetic solids: an experimental case study incorporating copper(II) amino acid complexes, J. Magn. Reson. 191 (2008) 31–46, https://doi.org/10.1016/j.jmr.2007.11.012.
[36] T. Sandreczki, D. Ondercin, R.W. Kreilick, Low-temperature NMR studies of a single crystal of trans-Cu(DL-ala)2.H2O, J. Am. Chem. Soc. 101 (1979) 2880–2884, https://doi.org/10.1021/ja00505a014.
[37] S.K. Kumara Swamy, A. Karczmarska, M. Makowska-Janusik, A. Kassiba, J. Dittmer, Solid-state NMR correlation experiments and distance measurements in paramagnetic metalorganics exemplified by Cu-cyclam, ChemPhysChem 14 (2013) 1864–1870, https://doi.org/10.1002/cphc.201300119.
[38] G. Szalontai, R. Csonka, G. Speier, J. Kaizer, J. Sabolović, Solid-state NMR study of paramagnetic bis(alaninato-κ ^{2} *N* , *O*)copper(II) and bis(1-amino(cyclo)alkane-1-carboxylato-κ ^{2} *N* , *O*)copper(II) complexes: reflection of stereoisomerism and molecular mobility in ^{13} C and ^{2} H fast magic angle spinning spectra, Inorg. Chem. 54 (2015) 4663–4677, https://doi.org/10.1021/ic502987e.
[39] M. Babinský, K. Bouzková, M. Pipíška, L. Novosadová, R. Marek, Interpretation of crystal effects on NMR chemical shift tensors: electron and shielding deformation densities, J. Phys. Chem. A. 117 (2013) 497–503, https://doi.org/10.1021/jp310967b.
[40] P. Schanda, M. Ernst, Studying dynamics by magic-angle spinning solid-state NMR spectroscopy: principles and applications to biomolecules, Prog. Nucl. Magn. Reson. Spectrosc. 96 (2016) 1–46, https://doi.org/10.1016/j.pnmrs.2016.02.001.